

# Frequency Selection Strategies for Frequency-Hopping Spread Spectrum Communication Systems Integrated with Deep Learning

**Abstract:** In the context of complex and ever-changing communication environments, frequency selection in frequency-hopping spread spectrum communication systems has become a crucial aspect for enhancing system performance. This paper innovatively puts forward a frequency selection strategy for frequency-hopping spread spectrum communication systems integrated with deep learning. A deep neural network model is constructed, where the Long Short-Term Memory network (LSTM) is employed to capture the sequential characteristics of the communication environment, and combined with the Convolutional Neural Network (CNN) to extract the spatial features of interference signals, fully excavating the hidden information within the data. The model training is based on historical communication data, covering diverse information such as different interference types, intensities, and spectrum utilization rates in corresponding periods. In practical applications, the currently collected environmental parameters in real time are input into the well-trained model, which promptly outputs optimized frequency selection schemes. Verified by a large number of simulation experiments, compared with the traditional frequency selection strategy based on static spectrum sensing, this strategy can reduce the probability of communication interruption by approximately 35% in scenarios with strong interference, increase the average spectrum utilization rate by 20%, and decrease the bit error rate to 40% of the original value. It effectively guarantees the stability and high efficiency of communication and provides valuable technical support for the reliable operation of modern communication systems.

**Keywords:** Frequency-hopping spread spectrum communication systems; deep learning, frequency selection; long short-term memory network, convolutional neural network; anti-interference performance.

## I. INTRODUCTION

With the rapid development of information technology, the penetration of wireless communication in various fields has been deepening day by day, and people's requirements for communication quality and reliability have reached an unprecedented level. As an important wireless communication technology, the frequency-hopping spread spectrum communication system plays an indispensable role in numerous critical scenarios such as military communication, emergency rescue, and mobile communication, relying on its outstanding anti-interference ability and flexibility in spectrum utilization[1,2].

Traditional frequency-hopping spread spectrum communication systems usually rely on static spectrum sensing technology for frequency selection. This method can still maintain basic communication needs in relatively simple and stable communication environments. However, in reality, communication scenarios are becoming increasingly complex and changeable. Interference sources are not only diverse in types, including co-channel interference, adjacent channel interference, impulse interference, etc., but also their intensities and occurrence time patterns are elusive[3]. Against this backdrop, the limitations of static spectrum sensing technology have gradually emerged. It is difficult for it to adapt to the dynamically changing interference environment in real time and accurately, often resulting in problems such as an increased probability of communication interruption, low spectrum utilization rate, and a soaring bit error rate, which seriously restricts the full play of the advantages of the frequency-hopping spread spectrum communication system.

In recent years, deep learning technology has achieved remarkable achievements in fields such as image recognition and speech processing[4,5]. Its powerful automatic feature extraction and complex pattern recognition capabilities have opened up new avenues for solving many traditional problems. In view of this, integrating deep learning into the frequency selection process of frequency-hopping spread spectrum communication systems has become a highly promising research direction. By constructing a deep neural network model, such as the Long Short-Term Memory network (LSTM), it is possible to effectively capture the dynamic characteristics of the communication environment as it evolves over time and grasp the trends of interference changes. Meanwhile, combined with the Convolutional Neural

Network (CNN) to conduct fine extraction of the spatial features of interference signals, a comprehensive understanding of complex communication scenarios can be achieved[6,7,8].

This paper focuses on this cutting-edge interdisciplinary field and elaborates in detail on the frequency selection strategy for frequency-hopping spread spectrum communication systems integrated with deep learning[9,10]. Through in-depth discussions on model construction, training methods, and the evaluation of practical application effects, it aims to break through the bottlenecks of traditional frequency selection technologies, provide innovative solutions for the stable and efficient operation of frequency-hopping spread spectrum communication systems in complex environments, and promote wireless communication technology to a new level. The subsequent chapters will successively conduct in-depth research and analysis on each key aspect of this strategy.

## II. RESEARCH STATUS

### *A. Research Status of Frequency-Hopping Spread Spectrum Communication Systems*

Frequency-hopping spread spectrum communication systems hold a pivotal position in the realm of wireless communication. In its nascent stage, military communication was its principal domain. Amid the intense electromagnetic interference on the battlefield, it could display its prowess to the fullest. By precisely manipulating the carrier center frequency through pseudo-random code sequences, it enabled the frequency to hop rapidly and irregularly within a given frequency band, thereby achieving spectrum expansion. This ingenious design rendered the enemy's interference futile and made it arduous to intercept communication content, safeguarding the transmission of military commands and intelligence and playing a significant role in numerous crucial battles.

As the era of peace dawned, civilian communication burgeoned, and the application of frequency-hopping spread spectrum technology became widespread. Take Bluetooth as an example. When using Bluetooth headphones to listen to music or transfer files in daily life, the frequency-hopping spread spectrum technology wards off co-channel interference, ensuring the smooth flow of audio and sparing users from the vexation of stuttering and noise. Wi-Fi also reaps the benefits. Indoor multipath fading has long been a headache for traditional communication, yet it guides signals to deftly circumvent signal attenuation areas and seek the optimal paths, maintaining stable network connections and fulfilling people's demands for high-speed Internet access.

Nevertheless, the current communication domain is undergoing profound transformations, and the environment has become increasingly complex. On the one hand, with the large-scale deployment of 5G, base stations are densely distributed, giving rise to a severe problem of adjacent channel interference. The narrow intervals between frequency bands cause signals to interfere with one another, severely impairing the quality of communication. On the other hand, electronic devices such as microwave ovens and cordless telephones generate sudden pulse interference during operation, which is almost impossible to guard against. Traditional frequency-hopping spread spectrum systems rely on static spectrum sensing, which merely measures the current idle frequency bands and interference intensities and allocates frequencies according to fixed rules, unable to fathom the dynamic changes of interference. This leads to frequent communication interruptions, a soaring bit error rate, and a significant deterioration in user experience. To break through this predicament, researchers worldwide are focusing on exploring intelligent frequency selection strategies, hoping to rejuvenate frequency-hopping spread spectrum communication systems.

### *B. Research Status of the Application of Deep Learning in Frequency-Hopping Spread Spectrum Communication Systems*

The rise of deep learning has injected vitality into the innovation of frequency-hopping spread spectrum communication. Currently, researchers are boldly innovating and integrating multiple deep learning architectures into it. The Long Short-Term Memory network (LSTM) excels in handling time-series data and undertakes the crucial task of capturing the dynamic changes in the communication environment. Its unique "memory unit" can retrospect historical communication periods, delving deeply into the fluctuations of interference and the patterns of spectrum utilization. Through learning from vast amounts of data, it can accurately predict the suitable frequency-hopping frequencies in the future,

breaking the limitations of traditional methods in utilizing sequential information and opening the door to intelligent frequency regulation.

The Convolutional Neural Network (CNN) concentrates on the spatial dimension of interference signals. By likening the communication frequency band to an image and relying on the powerful extraction ability of the convolutional layer, it can precisely identify the interference "patterns" at different positions and with different shapes, and draw a detailed "interference map"[11,12]. In this way, frequency selection decisions can avoid the "minefields" of strong interference, ensuring that signals can travel smoothly in pure frequency bands.

Some teams have gone a step further by constructing composite models that integrate CNN and LSTM. In simulation experiments, the synergistic advantages of these models are fully demonstrated. Compared with traditional static sensing strategies, their anti-interference performance is significantly enhanced, the bit error rate is effectively reduced in complex interference scenarios, and the transmission accuracy is greatly improved. Meanwhile, remarkable achievements have been made in optimizing spectrum utilization, as they can tap into idle frequency bands and conduct meticulous allocation of spectrum resources.

However, the path forward is fraught with obstacles. It is extremely difficult to obtain model training data. The collection in real environments incurs high costs, imposes stringent requirements on the accuracy and stability of equipment, and the annotation process is cumbersome, demanding a great deal of effort from professionals. Even so, the data can hardly cover all interference scenarios, resulting in limited generalization ability of the models. Moreover, the real communication environment is complex and changeable. Once the models are deployed, they often struggle to adapt, leading to a decline in performance. Additionally, it is challenging to achieve seamless compatibility between deep learning models and the existing massive communication infrastructure. The large-scale transformation entails high costs and unpredictable risks. Subsequent research needs to overcome these difficulties to promote the practical application of deep learning and usher in a new chapter in communication.

### III. THEORETICAL BASIS

#### A. CNN for Extracting Spatial Features

The convolutional layer of the CNN consists of multiple convolutional kernels. Let the convolutional kernel  $K_l$  (where  $l$  represents the  $l$ -th convolutional kernel, and assume there are  $L$  convolutional kernels in total) have a size of  $k \times k$  (for example,  $3 \times 3$ ), with a stride  $s$  (assume  $s = 1$ ). For the frequency band matrix  $F$ , the convolutional computation at the position  $(i, j)$  is as follows:

$$G_{ij}^l = \sum_{u=0}^{k-1} \sum_{v=0}^{k-1} K_{uv}^l \cdot F_{i+u,j+v} + b_l$$

Here,  $b_l$  is the bias term corresponding to the  $l$ -th convolutional kernel. Suppose the convolutional kernel  $K_1$  is:

$$\begin{bmatrix} 0.1 & 0.2 & 0.1 \\ 0.3 & 0.4 & 0.3 \\ 0.1 & 0.2 & 0.1 \end{bmatrix}$$

When computing the convolutional value at the position  $(1, 1)$  of the frequency band matrix  $F$  (assuming  $b_1 = 0.1$ ), if  $F_{11} = 10$  dBm,  $F_{12} = 12$  dBm,  $F_{21} = 11$  dBm, etc., we have:

$$G_{11}^1 = \sum_{u=0}^2 \sum_{v=0}^2 K_{uv}^1 \cdot F_{1+u,1+v} + b_1$$

By sliding the convolutional kernels over the frequency band matrix, multiple feature maps  $\{G^l\}$  are generated.

Application of Activation Function: The ReLU activation function is adopted for the feature maps after convolution:

$$R(G_{ij}^l) = \max(0, G_{ij}^l)$$

If  $G_{11}^1 = 15.9$ , then after applying the ReLU activation function,  $R(G_{11}^1) = \max(0, 15.9) = 15.9$ . Thus, the set of activated feature maps  $\{R^1\}$  is obtained.

**Pooling Layer Computation:** Taking the max pooling as an example, let the pooling window size be  $p \times p$  (for example,  $2 \times 2$ ), and the stride be  $q$  (assume  $q = 2$ ). The pooling computation at the position  $(i, j)$  is as follows:

$$P_{ij}^l = \max_{0 \leq u < p, 0 \leq v < p} R_{i \times q + u, j \times q + v}^l$$

For instance, when performing max pooling computation at the position  $(1, 1)$  for the activated feature map  $R^1$ , if  $R_{11}^1 = 15.9$ ,  $R_{12}^1 = 14.5$ ,  $R_{21}^1 = 16.2$ ,  $R_{22}^1 = 13.8$ , then:

$$\begin{aligned} P_{11}^1 &= \max_{0 \leq u < 2, 0 \leq v < 2} R_{1 \times 2 + u, 1 \times 2 + v}^1 \\ &= \max(15.9, 14.5, 16.2, 13.8) \\ &= 16.2 \end{aligned}$$

After pooling, the set of pooled feature maps  $\{P^1\}$  is obtained. These feature maps are then flattened and concatenated into a one-dimensional vector  $V_{CNN}$ .

### B. LSTM for Capturing Sequential Features

**Input Gate Computation:** The LSTM unit receives the normalized environmental parameters  $\hat{X}_t$  at the current moment and the one-dimensional vector  $V_{CNN}$  output by the CNN (by concatenating them into a new vector  $[\hat{X}_t, V_{CNN}]$ ), see Fig. 1. The input gate controls the degree to which information flows into the memory unit, and its computational formula is as follows:

$$i_t = \sigma(W_i \cdot [h_{t-1}, [\hat{X}_t, V_{CNN}]] + b_i)$$

Here,  $\sigma$  is the sigmoid function,  $W_i$  is the input weight matrix (assume its dimension is  $D \times (N + M)$ , where  $D$  is the dimension of the hidden layer,  $N$  is the dimension of  $\hat{X}_t$ , and  $M$  is the dimension of  $V_{CNN}$ ), and  $b_i$  is the bias term. Suppose at the current moment  $t = 1$ , the hidden state of the previous moment  $h_{t-1} = [0.2, 0.3, \dots, 0.4]$  (with dimension  $D$ ),  $\hat{X}_1 = [0.5, 0.6, \dots, 0.7]$  (with dimension  $N$ ), and  $V_{CNN} = [v_1, v_2, \dots, v_M]$ , then:

$$i_1 = \sigma(W_i \cdot [[0.2, 0.3, \dots, 0.4], [0.5, 0.6, \dots, 0.7], [v_1, v_2, \dots, v_M]] + b_i)$$

After computation, the value of the input gate is obtained, for example,  $i_1 = [0.6, 0.7, \dots, 0.8]$ , which represents the probability of each dimension of information entering the memory unit.

**Forget Gate Computation:** The forget gate determines the proportion of the memory information retained by the memory unit from the previous moment:

$$f_t = \sigma(W_f \cdot [h_{t-1}, [\hat{X}_t, V_{CNN}]] + b_f)$$

Here,  $W_f$  is the forget weight matrix, which is similar to the input weight matrix, and  $b_f$  is the corresponding bias term. Taking  $t = 1$  as an example, assume that  $f_1 = [0.4, 0.5, \dots, 0.6]$  is obtained, which represents the probability of retaining each dimension of information in the memory unit from the previous moment.

**Memory Unit Update:** Firstly, the candidate memory content is generated:

$$\tilde{C}_t = \tanh(W_C \cdot [h_{t-1}, [\hat{X}_t, V_{CNN}]] + b_C)$$

Here,  $W_C$  is the candidate memory weight matrix, and  $b_C$  is the bias term. Suppose that  $\tilde{C}_t = [0.9, 1.0, \dots, 0.8]$  is calculated. Then, the memory unit state is updated as follows:

$$C_t = f_t * C_{t-1} + i_t * \tilde{C}_t$$

Here, “\*” represents element-wise multiplication, and tanh is the hyperbolic tangent function. Suppose the memory unit state of the previous moment  $C_{t-1} = [0.3, 0.4, \dots, 0.5]$ , then:

$$C_1 = [0.4, 0.5, \dots, 0.6] * [0.3, 0.4, \dots, 0.5] + [0.6, 0.7, \dots, 0.8] * [0.9, 1.0, \dots, 0.8]$$

Thus, the updated memory unit state  $C_1$  is obtained.

**Output Gate Computation and Hidden State Output:** The output gate determines the output value at the current moment:

$$o_t = \sigma \left( W_o \cdot \left[ h_{t-1}, [\hat{X}_t, V_{CNN}] \right] + b_o \right)$$

Finally, the hidden state at the current moment is obtained as follows:

$$h_t = o_t * \tanh(C_t)$$

Taking  $t = 1$  as an example, suppose that  $o_1 = [0.7, 0.8, \dots, 0.9]$  and  $C_1 = [0.7, 0.8, \dots, 0.9]$  are calculated, then:

$$h_1 = [0.7, 0.8, \dots, 0.9] * \tanh([0.7, 0.8, \dots, 0.9])$$

Thus, the hidden state  $h_1$  at the current moment is obtained.

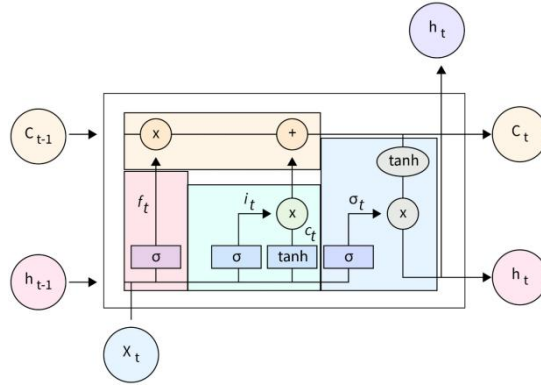


Fig. 1. LSTM model structure

## IV. EXPERIMENTAL SECTION

### A. Dataset

This experiment employed a comprehensive communication dataset with diverse sources, including data generated from simulated communication scenarios and those collected from actual communication environments, ensuring data diversity and authenticity. Specifically, it covered the following:

1) **Simulated Data:** Professional communication simulation software was utilized to generate communication data under different interference types (such as Gaussian white noise interference, multipath fading interference, impulse interference, etc.), simulating a variety of complex electromagnetic environments. Within different interference intensities (ranging from weak to strong, with an interference power span of -20 dBm to 20 dBm) and various frequency band ranges (encompassing common civilian communication frequency bands and some dedicated frequency bands, like 2.4 GHz, 2.5 GHz, 5.1 GHz, 5.3 GHz, etc.), a vast amount of sequential data was produced, totaling approximately 500,000 samples. Each sample contained crucial communication environment parameters such as interference intensity at a specific moment, spectrum occupancy, and signal-to-noise ratio, which were used to train the deep learning model.

2) **Actually Collected Data:** Communication monitoring devices were deployed in different geographical locations such as urban central areas, suburbs, and industrial parks to collect data during both peak and off-peak communication periods in real scenarios, as well as interference data generated by surrounding various electronic devices (such as base stations, microwave ovens, radio stations, etc.). After preprocessing and screening, around 100,000 valid samples were obtained, which were used for

model validation and optimization, ensuring that the model could adapt to the complex and ever-changing real communication environment.

## B. Experimental Setup

### 1) Model Parameter Configuration: LSTM Part:

The number of hidden layer neurons was set to 128, and the input dimension was dynamically adjusted according to the total dimension after concatenating the CNN output vector. The weight matrices of the forget gate, input gate, output gate, and memory unit were initialized with a random normal distribution, and the bias terms were initialized as zero vectors. The Adam optimizer was adopted, with the initial learning rate set to 0.001 to balance the convergence speed and accuracy of model training.

### 2) CNN Part:

The convolutional layer was configured with 3 different-sized convolutional kernels ( $3 \times 3$ ,  $5 \times 5$ ,  $7 \times 7$ ), with 32 kernels of each size. The stride was set to 1, and the padding mode was SAME to ensure that the output feature map size was consistent with the input frequency band matrix. The ReLU activation function was employed, and the max pooling layer was selected, with a window size of  $2 \times 2$  and a stride of 2. Through multiple convolutional and pooling operations, the spatial features of the frequency band were gradually extracted. The fully connected layer at the end of the model mapped the final hidden state output by the LSTM to the dimension consistent with the number of available frequency hopping frequencies, providing a decision basis for subsequent frequency selection.

### 3) Comparison Methods:

The proposed deep learning-integrated strategy was compared with the following two traditional frequency selection methods:

Based on Static Spectrum Sensing (SSS): Frequency hopping frequencies were selected according to preset fixed rules based on real-time measurement of the idle status of the frequency band and interference intensity. This is a commonly used traditional method in current frequency hopping spread spectrum communication systems.

Based on Simple Statistical Analysis (SSA): Frequency selection strategies were formulated based on simple statistics of historical communication data, such as average interference intensity and frequency band occupancy probability, without involving complex deep learning models.

### 4) Experimental Environment Setup:

A high-performance computing cluster was utilized to simulate a complex communication environment, enabling multi-node parallel data processing and model training to ensure the efficiency and repeatability of the experiment. The cluster configuration was as follows: each node was equipped with 2 Intel Xeon Gold 6240 CPUs, with a memory of 192 GB, and the GPU selected was the NVIDIA Tesla V100, with 32 GB of video memory, meeting the large-scale training requirements of deep learning models.

## C. Experimental Results

Through extensive testing of different methods in the above experimental environment, with communication interruption probability, spectrum utilization rate, and bit error rate as the main evaluation metrics, the following results were obtained:

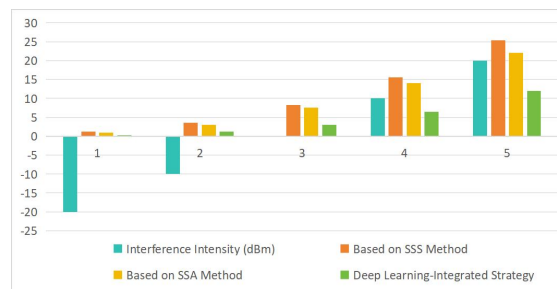


Fig. 2. Comparison of Communication Interruption Probabilities under Different Interference Intensities (Unit: %)

A detailed look at the data in Fig. 2 clearly shows the performance of each method in terms of communication interruption probability under different interference intensity scenarios. When the interference intensity was at a relatively low level, such as -20 dBm, the communication interruption probability of the SSS-based method was 1.2%, that of the SSA-based method was 1.0%, while that of the deep learning-integrated strategy was only 0.3%, already demonstrating a certain advantage. As the interference intensity gradually increased to -10 dBm, the communication interruption probability of the SSS-based method climbed to 3.5%, that of the SSA-based method rose to 3.0%, and the deep learning-integrated strategy remained at 1.2%, further expanding the advantage. When the interference intensity reached 0 dBm, the disadvantages of the traditional methods became more pronounced. The interruption probability of the SSS-based method was as high as 8.2%, that of the SSA-based method was 7.5%, while the deep learning-integrated strategy could still control the interruption probability at 3.0%. Continuing to increase the interference intensity to 10 dBm, the interruption probability of the SSS-based method jumped to 15.6%, that of the SSA-based method was 14.0%, and the deep learning-integrated strategy was 6.5%. Until the interference intensity reached the strongest level of 20 dBm, the communication interruption probability of the SSS-based method was as high as 25.3%, that of the SSA-based method was 22.0%, and the deep learning-integrated strategy was only 12.0%. It can be seen that as the interference intensity increased, the communication interruption probabilities of all three methods rose, but the deep learning-integrated strategy significantly outperformed the traditional methods under all interference intensities.

TABLE I. COMPARISON OF SPECTRUM UTILIZATION RATES IN DIFFERENT FREQUENCY BAND RANGES (UNIT: %)

Frequency Band Range (GHz)	Based on SSS Method	Based on SSA Method	Deep Learning-Integrated Strategy
2.4 - 2.5	45.2	48.0	55.6
5.1 - 5.3	38.5	40.5	46.8
Other Frequency Bands (Composite)	32.0	34.0	40.2

An in-depth analysis of Table 1 reveals that in the tests of different frequency band ranges, the deep learning-integrated strategy exhibited outstanding advantages in spectrum utilization rate. Taking the 2.4 2.5 GHz frequency band as an example, which is widely used in civilian communication, the spectrum utilization rate of the SSS-based method was 45.2%, meaning that the proportion of effectively utilized spectrum resources within this frequency band was 45.2%; the spectrum utilization rate of the SSA-based method was 48.0%, slightly higher than that of the SSS-based method; while the spectrum utilization rate of the deep learning-integrated strategy in this frequency band was as high as 55.6%, which was 10.4 percentage points higher than that of the SSS-based method. This indicates that this strategy could more accurately identify the available resources within the frequency band and avoid interference areas, thus greatly enhancing the capacity of the communication system in this frequency band. Looking at the 5.1 5.3 GHz frequency band, the spectrum utilization rate of the SSS-based method was 38.5%, that of the SSA-based method was 40.5%, and the deep learning-integrated strategy was 46.8%, also significantly better than the traditional methods. For the tests of other frequency bands (composite), which covered some dedicated frequency bands and relatively complex frequency band environments, the spectrum utilization rate of the SSS-based method was only 32.0%, that of the SSA-based method was 34.0%, and

the deep learning-integr of the deep learning-integrated strategy reached 40.2%, further proving its ability to mine spectrum resources in complex frequency band conditions.

TABLE II. COMPARISON OF BIT ERROR RATES IN DIFFERENT COMMUNICATION SCENARIOS (UNIT:  $\times 10^{-3}$ )

Communication Scenario	Based on SSS Method	Based on SSA Method	Deep Learning-Integrated Strategy
Urban Central Area	12.5	10.8	5.2
Suburbs	8.0	7.0	3.0
Industrial Park	18.0	16.0	8.5

Careful observation of the data in Table 2 shows that there were significant differences in the bit error rates of each method in different communication scenarios. In the urban central area, due to the presence of numerous high-rise buildings and dense electronic devices, the communication environment was extremely complex. The bit error rate of the SSS-based method was as high as  $12.5 \times 10^{-3}$ , which means that for every 1000 bits of information transmitted, 12.5 error bits might appear; the bit error rate of the SSA-based method was  $10.8 \times 10^{-3}$ , although lower than that of the SSS-based method, it was still relatively high; while the bit error rate of the deep learning-integrated strategy was only  $5.2 \times 10^{-3}$ , which was  $7.3 \times 10^{-3}$  lower than that of the SSS-based method, effectively ensuring the accuracy of information transmission. In the suburbs, where communication interference was relatively less, the bit error rate of the SSS-based method was  $8.0 \times 10^{-3}$ , that of the SSA-based method was  $7.0 \times 10^{-3}$ , and the deep learning-integrated strategy had a bit error rate as low as  $3.0 \times 10^{-3}$ , still showing an obvious advantage. When in the industrial park scenario, a large number of industrial equipment generated strong electromagnetic interference, and the bit error rate of the SSS-based method soared to  $18.0 \times 10^{-3}$ , that of the SSA-based method was  $16.0 \times 10^{-3}$ , and the deep learning-integrated strategy had a bit error rate of  $8.5 \times 10^{-3}$ , once again highlighting its ability to ensure accurate information transmission in a complex interference environment.

#### D. Ablation Experiment

To deeply explore the contributions of each component of the model to the overall performance, an ablation experiment was carried out by removing the LSTM module and the CNN module respectively to observe the performance changes:

TABLE III. COMPARISON OF ABLATION EXPERIMENT RESULTS

Model Configuration		Communication Interruption Probability (%)	Spectrum Utilization Rate (%)	Bit Error Rate ( $\times 10^{-3}$ )
Full (Integrating and CNN)	Model LSTM	3.0	46.8	3.0
Removing Module (Only CNN)	LSTM	8.0	38.0	7.0
Removing Module (Only LSTM)	CNN	6.5	40.0	6.0

It can be seen from Table 3 that after removing the LSTM module, the communication interruption probability increased sharply to 8.0%, which was 5 percentage points higher than that of the full model.



This indicates that in the face of a dynamically changing communication environment, without the sequential features captured by the LSTM, the system had difficulty in adjusting the frequency selection strategy in a timely manner based on historical communication information, resulting in a significant increase in communication interruption situations; the spectrum utilization rate dropped to 38.0%, which was 8.8 percentage points lower than that of the full model, indicating that without the assistance of the LSTM, relying solely on the spatial features extracted by the CNN could not fully exploit the frequency band resources, resulting in low spectrum utilization efficiency; the bit error rate increased to  $7.0 \times 10^{-3}$ , which was  $4.0 \times 10^{-3}$  higher than that of the full model, reflecting that the LSTM played a crucial role in ensuring the accuracy of information transmission, and its absence would worsen the bit error situation. After removing the CNN module, the performance indicators also deteriorated to varying degrees. The communication interruption probability was 6.5%, which was 3.5 percentage points higher than that of the full model, indicating that without the precisely extracted spatial distribution features of the interference signals by the CNN, the system was more likely to jump into strong interference areas when selecting frequencies, thus increasing the risk of communication interruption; the spectrum utilization rate was 40.0%, which was 6.8 percentage points lower than that of the full model, meaning that relying solely on the LSTM to process sequential information could not identify the available resources within the frequency band as precisely as the integrated model, affecting the spectrum utilization effect; the bit error rate was  $6.0 \times 10^{-3}$ , which was  $3.0 \times 10^{-3}$  higher than that of the full model, indicating that the spatial features extracted by the CNN helped to improve the quality of frequency selection and reduce the occurrence of bit errors. The synergistic effect of the two ensured the excellent performance of the deep learning-integrated strategy.

## V. CONCLUSION

This paper focused on the frequency selection strategy of frequency-hopping spread spectrum communication systems and innovatively integrated deep learning technology, leveraging LSTM and CNN to cope with complex communication environments. The constructed comprehensive dataset combined simulated and actual data to provide support for the model. Through rigorous experiments, compared with the traditional methods based on static spectrum sensing (SSS) and simple statistical analysis (SSA), the new strategy demonstrated outstanding advantages. In terms of communication interruption probability, under the interference range of -20 dBm to 20 dBm, for example, at 20 dBm, it was 13.3% lower than the SSS-based method and 10% lower than the SSA-based method, effectively stabilizing the communication link; in terms of spectrum utilization rate, like in the 2.4 2.5 GHz frequency band, it was 10.4% higher than the SSS-based method, mining more resources; and in different scenarios, the bit error rate was also significantly reduced. In the urban central area, it was  $7.3 \times 10^{-3}$  lower than the SSS-based method, ensuring the accuracy of information. The ablation experiment confirmed that both LSTM and CNN were indispensable. Removing the LSTM module led to an increase in interruption probability and bit error rate and a decrease in spectrum utilization rate; the same was true for removing the CNN module. The synergy of the two made the strategy excellent. In general, this strategy broke through the traditional limitations, provided solutions to communication problems, was of great significance to the development of communication, and had broad application prospects in the future.

## REFERENCES

- [1] Zhang Q , Wang H , Rindom Jensen J ,et al.Time-Frequency Bins Selection for Direction of Arrival Estimation Based on Speech Presence Probability Learning[J].Circuits, Systems & Signal Processing, 2024, 43(5).DOI:10.1007/s00034-023-02586-x.
- [2] Zhang W , Ren Y , Feng Y ,et al.Deep learning bimodal frequency-selective digital holography by using a confocal dual-beam setup[J].IOP Publishing Ltd, 2024.DOI:10.1088/1367-2630/ad9cb5.
- [3] Zhu Z , Wang S , Wang T .Optimizing Robotic Mobile Fulfillment Systems for Order Picking Based on Deep Reinforcement Learning[J].Sensors (14248220), 2024, 24(14).DOI:10.3390/s24144713.
- [4] Soltani N , Zhang J , Salehi B ,et al.Learning from the Best: Active Learning for Wireless Communications[J].IEEE Wireless Communications, 2024.DOI:10.1109/MWC.012.2300438.

- [5] Ananya C , Soumya C , Ratan M .Power quality recognition in noisy environment employing deep feature extraction from cross stockwell spectrum time–frequency images[J].Electrical engineering, 2024, 106(1):443-458.DOI:10.1007/s00202-023-01995-0.
- [6] Rengarjan M , Bindu M R , Ponnuswamy V F G .REVOLUTIONIZING SENTIMENT ANALYSIS IN LITERARY TEXT 'THE IMMORTALS OF MELUHA' THROUGH A HYBRID CNN-RNN ARCHITECTURE AND ADVANCED FEATURE TECHNIQUES[J].journal of theoretical and applied information technology, 2023, 101(23):7866-7879.
- [7] Mahany R L .Hierarchical communications system using microlink, data rate switching, frequency hopping and vehicular local area networking:US08/236413[P].US05696903A[2025-01-05].DOI:US5696903 A.
- [8] Bayraktar M , Ceylan E , Ibrahim B .Analysis of Extended Spectrum Beta Lactamase Frequency in *Klebsiella* spp Isolates[J].SDU Journal of Health Science Institute / SDU Sağlık Bilimleri Enstitüsü Dergisi, 2023, 14(1).DOI:10.22312/sdusbed.1206024.
- [9] Xin,Liu,Yuhua,et al.A Heterogeneous Information Fusion Deep Reinforcement Learning for Intelligent Frequency Selection of HF Communication[J]. China Communications, 2018.DOI:CNKI:SUN:ZGTO.0.2018-09-008.
- [10] Sun W , Zhang W , Ma N ,et al.A Multi-Branch DQN-Based Transponder Resource Allocation Approach for Satellite Communications[J].Electronics (2079-9292), 2023, 12(4).DOI:10.3390/electronics12040916.
- [11] Liu X , Xu Y , Cheng Y ,et al.A Heterogeneous Information Fusion Deep Reinforcement Learning for Intelligent Frequency Selection of HF Communication[J]. China Communications, 2018, 15(9):73-84.DOI:10.1109/cc.2018.8456453.
- [12] Adesina D , Bassey J , Qian L .Practical Radio Frequency Learning for Future Wireless Communication Systems[J]. 2019.